Ruthenium alkynyl, carbene and alkenyl complexes containing pendant uracil groups: an investigation into the formation of alkenyl-phosphonio complexes†

Michael J. Cowley, Jason M. Lynam,* Robert S. Moneypenny, Adrian C. Whitwood and Alastair J. Wilson

Received 30th June 2009, Accepted 17th August 2009
First published as an Advance Article on the web 18th September 2009
DOI: 10.1039/b912855g

The vinylidene complex [Ru(η^5-C_5H_5)(PPh_3)$_2$(=C=CHUr)][X] (X = PF_6, OTf, Ur = uracil) is a versatile precursor for a range of organometallic complexes containing pendant uracil groups. Using appropriate conditions the vinylidene complex may be selectively transformed into alkynyl Ru(–C≡CUr)(η^5-C_5H_5)(PPh_3)$_2$, carbene [Ru(η^5-C_5H_5)(PPh_3)$_2$(=C{OMe}–CH_2Ur)][X] and alkenyl-phosphonio species [Ru(*E*-CH=C{PPh_3}Ur)(η^5-C_5H_5)(PPh_3)$_2$][X]. The synthesis of the related alkenyl-phosphonio complexes [Ru(*E*-CH=C{PPh_3}R)(η^5-C_5H_5)(PPh_3)$_2$][X] (R = Ph, C_6H_4-3-OMe) is described; these undergo a further orthometallation reaction: the mechanism of this latter reaction appears to proceed *via* dissociation of a ruthenium-bound PPh_3 ligand.

Introduction

The structure and reactivity of transition metal complexes containing vinylidene ligands continue to attract considerable interest.[1] Underlying the potential applications of these species is the fact that many electron-rich transition metal complexes may facilitate the isomerisation of terminal alkynes into their vinylidene tautomers.[2] The vinylidene ligands exhibit markedly different reactivity patterns when compared to the parent terminal alkynes[3] – notably, the α-carbon of the vinylidene is susceptible to nucleophilic attack and the β-carbon reacts with electrophiles.

This rich reactivity means that vinylidenes may act as synthons to metal complexes which contain carbene, carbyne or carbonyl ligands.[4] In addition, the β-carbon of vinylidene ligands in cationic complexes may be easily deprotonated to afford alkynyl complexes,[5] which are themselves important building blocks in, for example, materials with interesting electronic and non-linear optical properties.[6]

We have recently been engaged in a programme of research focused on utilising pendant nucleobase groups to direct the self-assembly of inorganic compounds in both the solid state and solution.[7] For example we have demonstrated that the reaction of RuCl(η^5-C_5H_5)(PPh_3)$_2$, **1**, with the uracil(Ur)-substituted alkyne HC≡CUr, **2**, in the presence of NH_4X (X = BF_4, PF_6, OTf) results in the formation of vinylidene complexes [Ru(η^5-C_5H_5)(PPh_3)$_2$(=C=CHUr)][X], **3a**[X].[8] A related synthetic procedure was employed to prepare the isoelectronic complex [Mo(=C=CHUr)(η^7-C_7H_7)(dppe)][BF_4]. Importantly, the salts of **3a**$^+$ self-assemble in the solid state to form cyclic rosette containing six ruthenium cations, the assembly being mediated by hydrogen bonding interactions from the pendant uracil groups.

As vinylidene complexes structurally related to **3a**[X] have been shown to be versatile synthons for a range of organometallic species,[9,10] it was anticipated that a range of uracil-containing complexes could be derived from **3a**[X]. In particular, it is of interest to explore the factors controlling the assembly of the nucelobase-containing compounds in both the solid state and solution and if the presence of a functionalised substituent within the complex will have a pronounced effect on their chemistry.

We now report that **3a**[X] may act as a precursor to complexes containing alkynyl, Ru(–C≡CUr)(η^5-C_5H_5)(PPh_3)$_2$, **4a**, carbene [Ru(η^5-C_5H_5)(PPh_3)$_2$(=C{OMe}-CH_2Ur)][X], **5a**[X] and alkenyl-phosphonio, [Ru(*E*-CH=C{PPh_3}Ur)(η^5-C_5H_5)(PPh_3)$_2$][X], **6a**[X], ligands. Given the somewhat serendipitous isolation of **6a**[X], we have also investigated the preparation of complexes [Ru(*E*-CH=C{PPh_3}R)(η^5-C_5H_5)(PPh_3)$_2$][OTf] (R = Ph, **6b**[OTf]; R = C_6H_4-3-OMe, **6c**[OTf]). The synthesis and structure of **5a**[PF_6] has been reported in a preliminary communication.[11]

Results and discussion

The synthetic routes and structures of the complexes prepared in this study are shown in Scheme 1. The structures of complexes **5a**[OTf], **6a**[OTf], **6b**[OTf], and **6c**[OTf] have been determined by single crystal X-ray diffraction, selected bond lengths and angles are given in Table 1 and details of the data collections and structural refinements in Table 2. As part of this study the structure of the novel complex **3c**[OTf] was also determined: see ESI.†

a. Preparation and characterisation of Ru(–C≡CUr)(η^5-C_5H_5)(PPh_3)$_2$, 4a

Deprotonation of cationic ruthenium vinylidene complexes has proven to be a general and versatile route for the synthesis of alkynyl (Ru–C≡C–R) complexes. We therefore believed that a similar reaction of **3a**$^+$ could occur to give the neutral species Ru(–C≡CUr)(η^5-C_5H_5)(PPh_3)$_2$, **4a**.[9] Although the two N–H groups in the uracil could, in principle, also be deprotonated by

Department of Chemistry, University of York, Heslington, York, UK YO10 5DD. E-mail: jml12@york.ac.uk; Fax: +44 (0)1904 432516; Tel: +44 (0)1904 432534

† Electronic supplementary information (ESI) available: $^{31}P\{^1H\}$ NMR simulations for **6c**[OTf] and $^1H\{^{31}P\}$ NMR experiments. CCDC reference numbers 737832 (**3c**[OTf]), 737833 (**5a**[OTf]), 737834 (**6a**[OTf]), 737835 (**6b**[OTf]) and 737836 (**6c**[OTf]). For ESI and crystallographic data in CIF or other electronic format see DOI: 10.1039/b912855g

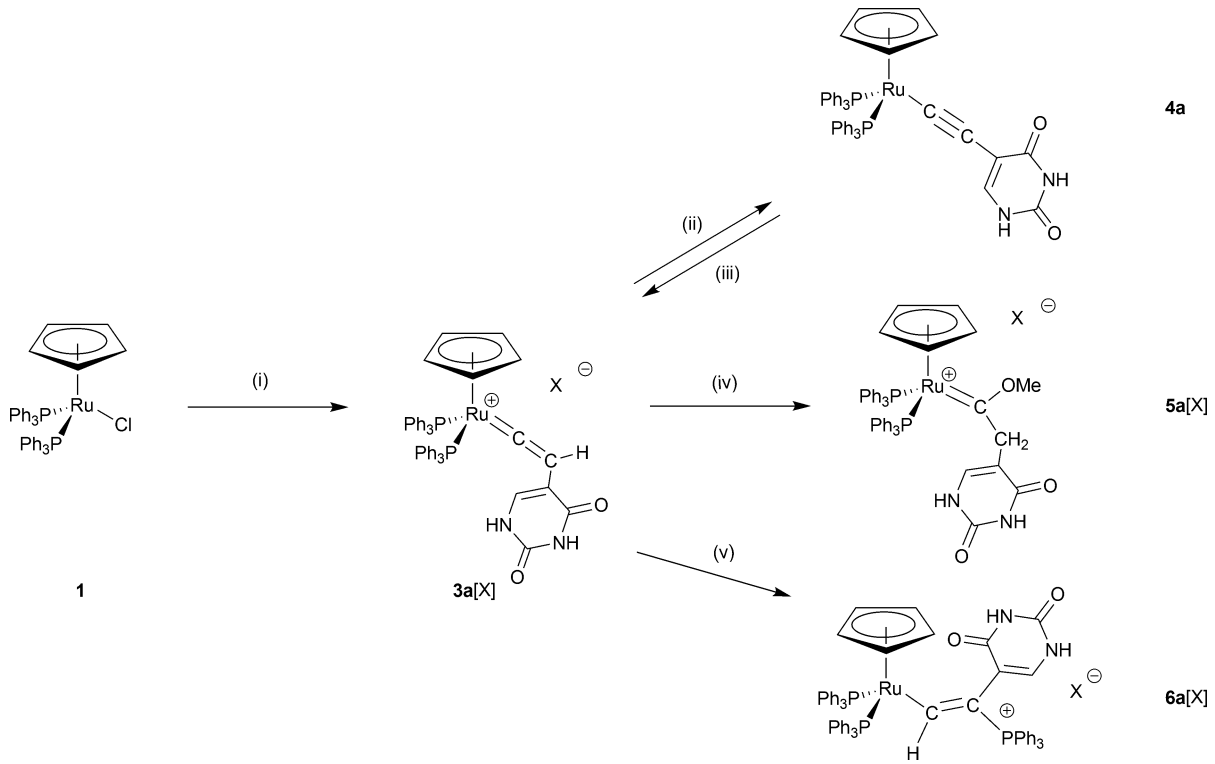

Scheme 1 Synthetic pathways employed in this study. (i) $+NH_4X$, **+2**, MeOH, $-NH_4Cl$; (ii) +NaOMe, –NaX, MeOH; (iii) $+H^+$; (iv) MeOH; (v) excess PPh_3, CH_2Cl_2, reflux; X = PF_6, OTf.

Table 1 Selected bond lengths (Å) and angles (°) for **5a**[OTf], **6a**[OTf], **6b**[OTf], and **6c**[OTf]; * indicates an intermolecular distance

	5a[OTf]	**6a**[OTf]	**6b**[OTf]	**6c**[OTf]
Ru(1)–P(1)	2.3220(4)	2.3172(15)	2.3271(8)	2.3289(15)
Ru(1)–P(2)	2.3444(4)	2.3375(14)	2.3354(8)	2.3232(15)
Ru(1)–C(1)	2.2849(18)	2.239(5)	2.242(3)	2.235(5)
Ru(1)–C(2)	2.2345(18)	2.238(5)	2.252(3)	2.242(6)
Ru(1)–C(3)	2.2521(18)	2.265(5)	2.254(3)	2.256(5)
Ru(1)–C(4)	2.2480(17)	2.243(5)	2.245(3)	2.241(5)
Ru(1)–C(5)	2.2665(17)	2.238(5)	2.257(2)	2.240(5)
Ru(1)–C(6)	1.9541(17)	2.063(5)	2.090(2)	2.070(5)
C(6)–C(7)	1.527(2)	1.377(6)	1.357(3)	1.366(7)
C(6)–O(1)	1.319(2)			
C(7)–(P3)		1.788(5)	1.798(3)	1.791(5)
N(2)–H(2A)···O(3)*	2.862(2)	2.796(5)		
P(1)–Ru(1)–P(2)	103.585(16)	102.06(5)	101.96(3)	101.98(5)
P(1)–Ru(1)–C(6)	90.91(5)	90.40(15)	90.75(7)	89.57(16)
P(2)–Ru(1)–C(6)	88.33(5)	89.23(13)	90.06(7)	91.14(14)

a strong base, it was anticipated that the vinylidene proton would in fact be the most acidic in the system[12] and that protection of the N–H groups of the uracil would not be necessary. This proved to be the case. Addition of 1 equivalent of NaOMe to a methanol solution of **3a**$^+$ resulted in a rapid colour change from deep red to bright yellow. Precipitation with hexane afforded a bright yellow microcrystalline complex, **4a**, which proved to be air stable in both the solid state and solution.

Complex **4a** was characterised by NMR and infra-red spectroscopy coupled with mass spectrometery: to date a single crystal suitable for study by X-ray diffraction has not been obtained. Furthermore due to its poor solubility, complete purification of **4a** proved troublesome, with the product always contaminated with $NaPF_6$.

The infra-red spectrum of **4a** exhibits a band at 2073 cm^{-1} which is in the region characteristic of the C≡C stretch of half-sandwich ruthenium alkynyl complexes.[9] Consistent with the formulation of **4a**, a peak was observed in the FAB mass spectrum at *m*/*z* 826. Importantly, the formation of **4a** from **3a**$^+$ is reversible: protonation with HCl or $HBF_4{\cdot}OEt_2$ in MeOH solution simply resulted in reformation of **3a**$^+$. Indeed, it proved possible to perform several protonation/deprotonation cycles on **4a** using $HBF_4{\cdot}OEt_2$/NaOMe with no apparent decomposition of the products. In this respect **4a** mirrors exactly the reactivity of Ru(–C≡CPh)(η^5-C_5H_5)(PPh_3)$_2$.[9]

The ^1H and $^{31}P\{^1H\}$ NMR spectra of **4a** in CD_2Cl_2 solution proved to be extremely complex—in the ^1H NMR spectrum, very broad resonances were observed in the aromatic region (for the phenyl rings of the coordinated phosphines) and for the cyclopentadienyl ligand. The $^{31}P\{^1H\}$ NMR spectrum exhibited a single very broad resonance. We suspected this broadness was due to the aggregation of **4a** in solution.

An NMR study employing CD_2Cl_2 solutions of **4a** prepared at a range of concentrations supported this argument. The $^{31}P\{^1H\}$ NMR spectrum of a 21.8 mM CD_2Cl_2 solution exhibited a single extremely broad resonance at δ 49.61 ($\omega_{\frac{1}{2}}$ = 1430 Hz). Systematically decreasing the concentration of this solution resulted in a narrowing of the resonance (Table 3). However, even at a concentration of 1.0 mM a linewidth of 917 Hz was observed. The NH resonances were not observed at any concentrations employed.

Table 2 Crystallographic data for complexes **3c**[OTf]·0.75CH_2Cl_2·0.25Et_2O, **5a**[OTf]·C_7H_8, **6a**[OTf], **6b**[OTf]·CH_2Cl_2, **6c**[OTf]·0.625CH_2Cl_2

	3c[OTf]·0.75CH_2Cl_2·0.25Et_2O	**5a**[OTf]·C_7H_8	**6a**[OTf]	**6b**[OTf]·CH_2Cl_2	**6c**[OTf]·0.56CH_2Cl_2
Empirical formula	$C_{52.75}H_{47}Cl_{1.50}F_3O_{4.25}P_2RuS$	$C_{56}H_{51}F_3N_2O_6P_2RuS$	$C_{66}H_{54}F_3N_2O_5P_3RuS$	$C_{69}H_{58}Cl_2F_3O_3P_3RuS$	$C_{69.56}H_{59.11}Cl_{1.11}F_3O_4P_3RuS$
Formula weight	1054.15	1100.06	1238.15	1289.09	1281.43
T/K	110(2)	150(2)	110(2)	110(2)	110(2)
Wavelength/Å	0.71073	0.71073	0.71073	0.71073	0.71073
Crystal system	Monoclinic	Triclinic	Monoclinic	Triclinic	Triclinic
Space group	$P2_1/n$	$P\bar{1}$	$P2_1/n$	$P\bar{1}$	$P\bar{1}$
a/Å	12.3192(10)	11.6129(5)	13.375(2)	10.2678(14)	10.3173(14)
b/Å	12.4402(10)	14.4787(6)	18.319(3)	14.522(2)	14.380(2)
c/Å	31.194(3)	15.9001(6)	23.489(4)	20.112(3)	20.203(3)
α [°]	90	95.010(1)	90	82.415(3)	82.335(3)
β [°]	94.150(2)	92.914(1)	101.392(4)	88.372(3)	88.087(3)
γ [°]	90	108.150(1)	90	80.570(3)	80.744(3)
Volume/Å^3	4768.1(7)	2522.10(18)	5641.5(16)	2932.5(7)	2931.7(7)
Z	4	2	4	2	2
Density (calculated) [Mg m^{-3}]	1.468	1.449	1.458	1.460	1.459
Absorption coefficient [mm^{-1}]	0.582	0.480	0.464	0.535	0.496
F(000)	2160	1132	2544	1324	1318.2
Crystal size/mm	0.21 × 0.12 × 0.09	0.20 × 0.19 × 0.15	0.18 × 0.04 × 0.03	0.30 × 0.12 × 0.01	0.20 × 0.05 × 0.03
Theta range for data collection [°]	1.31 to 28.32	1.49 to 30.02	1.42 to 25.09	1.86 to 28.35	1.02 to 22.61
Index ranges	$-16 \le h \le 16$ $-16 \le k \le 16$ $-41 \le l \le 41$	$-16 \le h \le 16$ $-19 \le k \le 20$ $-22 \le l \le 22$	$-15 \le h \le 15$ $-21 \le k \le 21$ $-27 \le l \le 22$	$-13 \le h \le 13$ $-18 \le k \le 19$ $-26 \le l \le 26$	$-11 \le h \le 11$ $-15 \le k \le 15$ $-21 \le l \le 21$
Reflections collected	48327	38454	31806	26119	18538
Independent reflections	11871 [R(int) = 0.0386]	14406 [R(int) = 0.0207]	9957 [R(int) = 0.1291]	14178 [R(int) = 0.0354]	7692 [R(int) = 0.0670]
Completeness (to theta)	99.8 (to 28.32°)	97.7 (to 30.02°)	99.4 (to 25.09°)	96.8 (to 28.35°)	98.9 (to 22.61°)
Absorption correction	Semi-empirical from equivalents				
Max. and min. transmission	0.950 and 0.843	0.977 and 0.848	0.986 and 0.789	0.950 and 0.687	0.985 and 0.880
Refinement method	Full-matrix least-squares on F^2				
Data/restraints/parameters	11871/4/635	14406/12/738	9957/0/730	14178/0/739	7692/1/779
Goodness-of-fit on F^2	1.057	1.035	0.954	1.003	1.044
Final R indices [$I > 2\sigma(I)$]	$R_1 = 0.0334$ w$R_2 = 0.0767$	$R_1 = 0.0351$ w$R_2 = 0.0889$	$R_1 = 0.0530$ w$R_2 = 0.0951$	$R_1 = 0.0428$ w$R_2 = 0.0959$	$R_1 = 0.0503$ w$R_2 = 0.1093$
R indices (all data)	$R_1 = 0.0447$ w$R_2 = 0.0810$	$R_1 = 0.0411$ w$R_2 = 0.0924$	$R_1 = 0.1234$ w$R_2 = 0.1175$	$R_1 = 0.0716$ w$R_2 = 0.1062$	$R_1 = 0.0784$ w$R_2 = 0.1213$
Largest diff. peak and hole/e Å^{-3}	0.660 and -0.523	1.083 and -0.625	0.736 and -0.971	1.311 and -1.017	0.675 and -0.652

Table 3 Effect of concentration on the appearance of the $^{31}P\{^1H\}$ NMR spectra of CD_2Cl_2 solutions of **4a**

[**4a**]/mM	Linewidth/Hz
1.0	917
4.4	1025
10.9	1241
21.8	1430

Employing d_6-DMSO as solvent resulted in spectra which were considerably sharper. For example, in the ^1H NMR spectrum distinct resonances were observed for the cyclopentadienyl, phenyl and uracil groups, however, once again the NH resonances could not be observed. A singlet at δ 49.44 in the $^{31}P\{^1H\}$ NMR spectrum was assigned to the PPh_3 ligands.

The fact that dissolution in DMSO afforded sharp resonances is consistent with little or no aggregation effects occurring in this solvent, therefore the ^1H and $^{31}P\{^1H\}$ NMR spectra of a 6.0 mM solution of **4** in a range of d_6-DMSO/CD_2Cl_2 solvent mixtures was studied. As can be seen from Table 4, even in 75% CD_2Cl_2/25% d_6-DMSO the linewidth is much narrower, indicating that aggregation is significantly reduced. On increasing the proportion of d_6-DMSO to 50%, two overlapping broad singlets were observed at δ 49.58 and δ 49.51. These singlets persisted, with changes in chemical shift, in the 75% d_6-DMSO solvent mixture. The presence of two separate resonances means that under these conditions there are at least two different hydrogen-bonded species in slow exchange, although each resonance could be due to many species in fast exchange. The fact that a single, sharp resonance is observed in pure d_6-DMSO is consistent with the presence of a monomeric species.

These results clearly indicate that the degree of aggregation of **4a** occurring in CD_2Cl_2 solution is considerable. The possible complementary hydrogen bonding patterns available to the uracil

Table 4 Effect of solvent on the appearance of the $^{31}P\{^1H\}$ NMR spectra of solutions of **4a** (6.0 mM)

% CD_2Cl_2/d_6-DMSO	δ	Linewidth/Hz
100/0	49.2	1160
75/25	49.58, 49.51	29
50/50	49.64, 49.56	—
25/75	49.44	—
0/100	49.44	6

group in dimeric species, along with the labelling scheme for the uracil group, are illustrated in Fig. 1. In the case of the vinylidene complex **3a**$^+$ we were able to obtain evidence that aggregation occurred to give dimeric species and the possible occurrence of all the potential hydrogen bonding aggregates **A**–**F**.[8] These data point to a more complex behaviour in the case of **4a** which, due to our inability to observe the N–H resonances in the ^1H NMR spectra, we have been unable to deconvolute further.

b. Preparation and characterisation of [Ru(η^5-C_5H_5)(PPh$_3$)$_2$(=C{OMe}–CH$_2$Ur)][X], 5[X]

Heating a methanol solution of **3a**[X] results in near quantitative conversion to the corresponding carbene complexes **5a**[X]. Indeed the conversion of **3a**[X] to **5a**[X] is extremely facile and even occurs in the solid state: mild heating of crystals of **3a**[X] (which are obtained as a MeOH solvate)[8] results in conversion to **5a**[X]. The most convenient synthesis of **5a**[X] is to perform prolonged (16 h) reactions of **1** with **2** and NH_4X in MeOH solution.

The solid state structure of both **5a**[PF_6][11] and **5a**[OTf] have been confirmed by single crystal X-ray diffraction. Slow cooling of a methanol–toluene solution of the salts allowed for isolation of crystals of the complexes as toluene solvates suitable for study by X-ray diffraction. The resulting structural determination (Fig. 2) illustrated that **5a**[PF_6] and **5a**[OTf] are essentially isostructural. The bond lengths and bond angles within the **5a**$^+$ cationic units are essentially identical and show, for example, short Ru=C distances (**5a**[PF_6] = 1.946(3) Å, **5a**[OTf] = 1.9541(17) Å). The cationic units in these species form hydrogen-bonded dimers involving a symmetric donor/acceptor interaction between N–H(2A) and C=O(3) with slightly shorter NH···O distance in **5a**[OTf] (**5a**[PF_6] = 2.897(3) Å, **5a**[OTf] = 2.862(2) Å). In both cases the N–H(1) group is engaged in hydrogen bonding to the respective anions (N–H···OTf 2.861(2) Å, N–H···FPF_5 3.005(3) Å). The OTf anion in **5a**[OTf] is disordered over two sites which differ in their arrangement relative to the plane containing the two hydrogen-bonded uracil groups.

The extent of the similarity between the structures observed for **5a**[PF_6] and **5a**[OTf] demonstrates that the formation of hydrogen bonds between pendant uracils on adjacent molecules is a general structural feature of these compounds and not just a consequence of crystal packing in a single example.

Evidence for the formation of aggregates of **5a**$^+$ in solution was obtained from the N–H resonances in ^1H NMR spectra. In CD_2Cl_2 solution these resonances exhibit significant concentration[11] and temperature dependence (Fig. 3). In general, an increase in the concentration of the solution or a decrease in the temperature both result in a shift of the N–H protons to lower field, behaviour

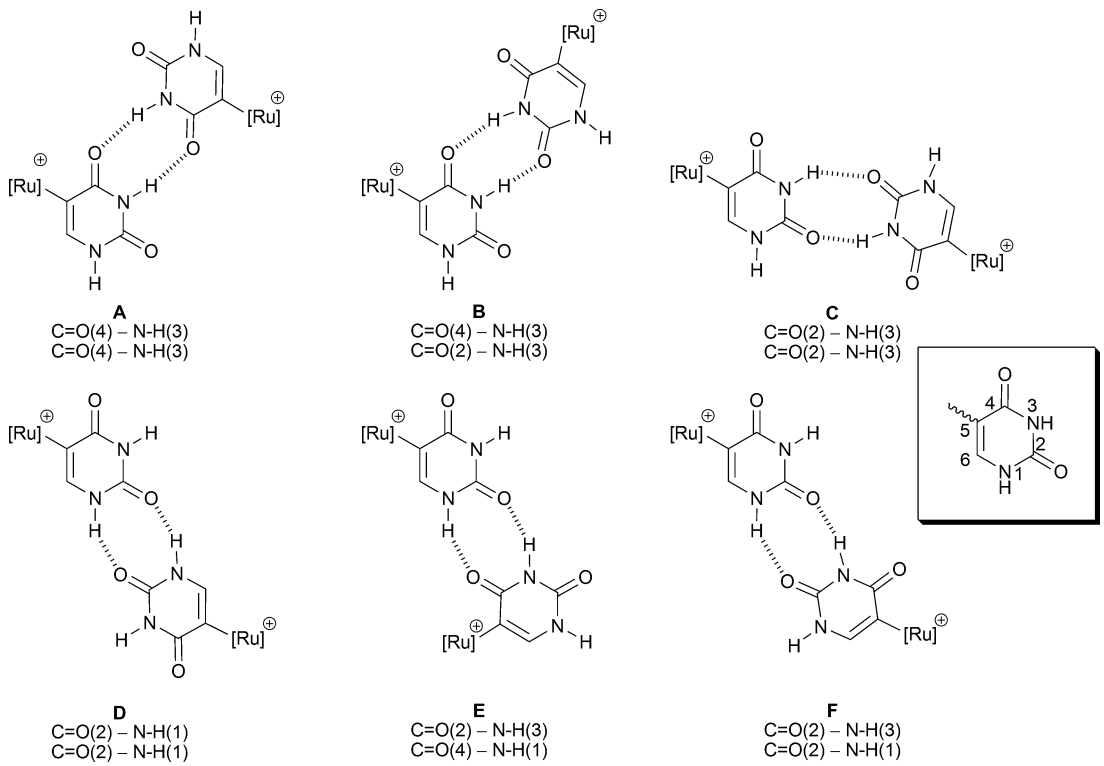

Fig. 1 Dimeric hydrogen-bonding patterns in solution. "C=O(4) – N–H(1)" refers to the hydrogen bonded motif exhibited by the uracil groups. [Ru]$^+$ = [Ru(η^5-C_5H_5)(PPh$_3$)$_2$(=C=C{H})]$^+$ (**3a**), Ru(–C≡C)(η^5-C_5H_5)(PPh$_3$)$_2$ (**4a**), [Ru(η^5-C_5H_5)(PPh$_3$)$_2$(=C{OMe}–CH$_2$)]$^+$ (**5a**$^+$), [Ru(CH=C{PPh$_3$})(η^5-C_5H_5)(PPh$_3$)$_2$]$^+$ (**6a**).

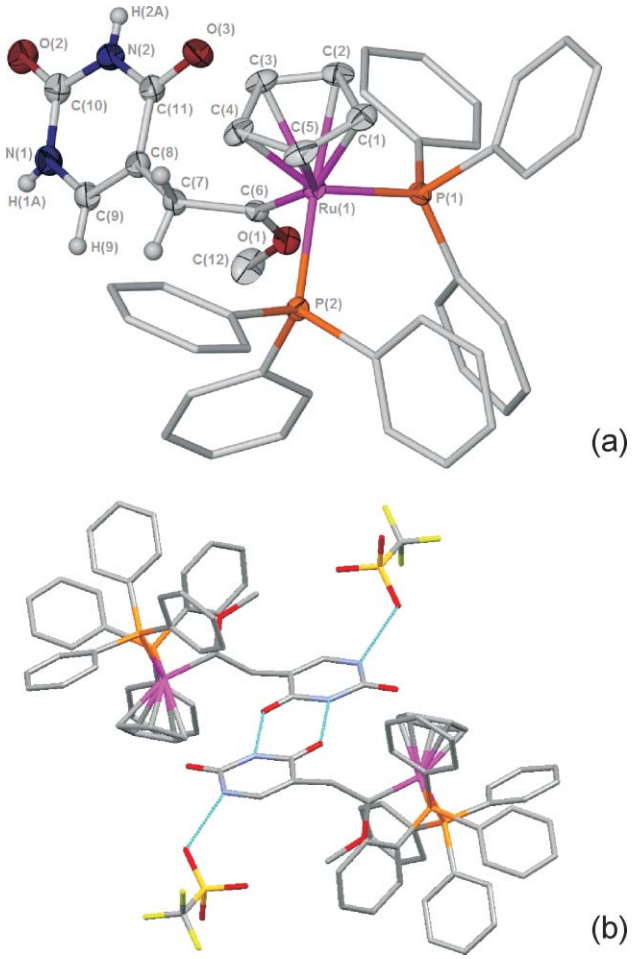

Fig. 2 (a) Structure of the cation of **5a**[OTf]. Selected thermal ellipsoids shown at the 50% probability level and selected hydrogen atoms omitted for clarity. (b) Hydrogen bonding motif observed in the solid state, only one orientation of the OTf anion shown.

that is typical of the formation of hydrogen-bonded aggregates. In general, the lower field N–H proton in unsubstituted uracil groups is assigned to N–H(3), the higher field N–H proton to N–H(1).[13] As may be observed in Fig. 3, increasing the concentration (or decreasing the temperature) of samples of **5a**[X] results in the resonances for both N–H(1) and N–H(3) moving to lower field, consistent with enhanced aggregation occurring. In addition, the resonance for N–H(1) shows a relatively smaller change in chemical shift when compared with N–H(3), implying that hydrogen bonding principally occurs through binding modes such as **A**–**C** (Fig. 1) with a smaller contribution from **D**–**F**.

c. Preparation and characterisation of β-alkenyl-phosphonio salts [Ru(*E*-CH=C{PPh$_3$}R)(η^5-C$_5$H$_5$)(PPh$_3$)$_2$][X], 6a[X]

Identification of the β-alkenyl-phosphonio complex 6a[OTf]. During our attempts to develop the synthesis of **5a**[OTf], we serendipitously discovered that the β-alkenyl-phosphonio complex **6a**[OTf] was a minor product formed in the reaction of **1** with **2** and NH_4OTf in MeOH at reflux. On one occasion, crystallisation of the reaction mixture afford a small crop of yellow crystals which a single crystal X-ray diffraction study demonstrated were the alkenyl-phosphonio complex [Ru(*E*-CH=C{PPh$_3$}Ur)(η^5-C$_5$H$_5$)(PPh$_3$)$_2$][OTf], **6a**[OTf].

The resulting structure determination (Fig. 4) demonstrated that the complex contains a half sandwich ruthenium Ru(η^5-C$_5$H$_5$)(PPh$_3$)$_2$ fragment coordinated to a alkenyl ligand, which is substituted at the β-position with both PPh$_3$ and Ur groups; the stereochemistry at the alkenyl ligand is *E*, *i.e.* with a *trans* disposition of Ru and PPh$_3$ groups. The bond metrics within the alkenyl fragment are discussed below. The uracil groups forms symmetric dimers, mediated by hydrogen bonding between N–H(3) and C=O(4). This motif is essentially identical to that shown by the carbene cations **5a**$^+$: however, the interaction between the nucleobases appears to be stronger in the case of **6a**$^+$ than **5a**$^+$ (N–H···O distance in **5a**[OTf] = 2.862(2) Å compared

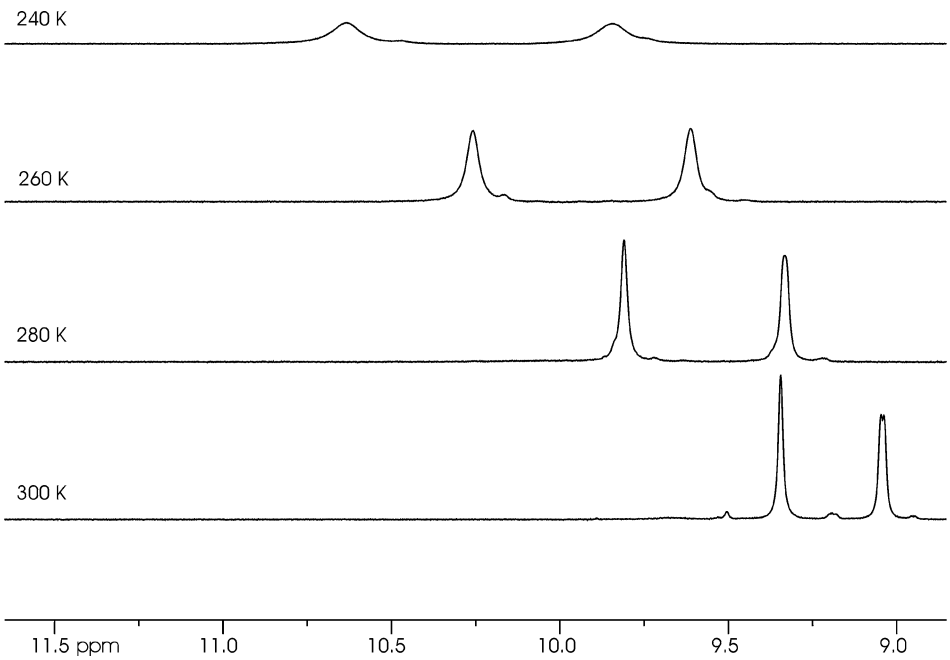

Fig. 3 (a) N–H region of ^{1}H NMR spectra of **5a**[OTf] recorded at various temperatures.

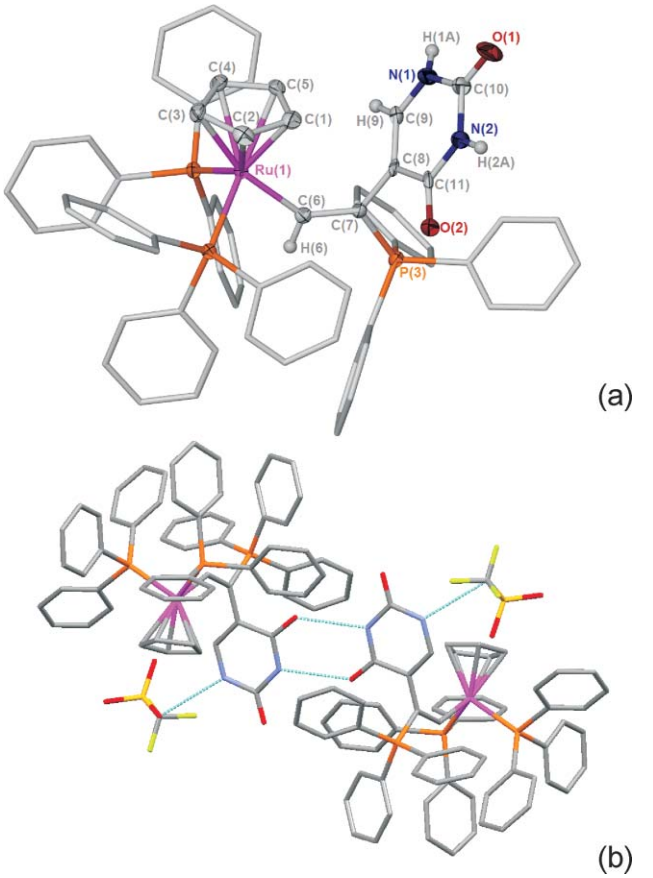

Fig. 4 (a) ORTEP representation of the structure of the cation of **6a**[OTf]. Selected thermal ellipsoids shown at the 50% probability level. Hydrogen atoms omitted for clarity. (b) Packing diagram showing hydrogen bonding interactions.

to 2.796(5) Å in **6a**[OTf]). Also, as in the case of **5a**$^+$, N–H(1) is involved in hydrogen bonding to the OTf anion (N–H $\cdots$ O = 2.796(5) Å).

General synthesis and characterisation of alkenyl-phosphonio complexes. Having identified **6a**[OTf] as a minor product in the reaction of **1** with **2** and NH_4OTf in MeOH a general synthetic route to complexes of this type was sought. Related ruthenium complexes with alkenyl-phosphonio ligand have been reported which contain indenyl[14,15] and cymene groups.[16] In addition, isoelectronic species $[M(\eta^5\text{-}C_5Me_5)(E\text{-}C(H)=C\{PPh_3\}Ph)(PR_3)(Cl)]^+$ (M = Rh or Ir), have been described.[16] The synthesis of these species involves either the reaction of an isolated vinylidene complex or the reaction between a metal complex with a terminal alkyne and PPh_3. To the best of our knowledge, the corresponding complexes $[Ru(E\text{-}CH=C\{PPh_3\}R)(\eta^5\text{-}C_5H_5)(PPh_3)_2]$, **6**$^+$, have not been observed previously. Therefore the development of a suitable synthetic route to these species with a range of substituents was an important goal so that the precise effects of the uracil group could be quantified.

Reaction of the vinylidene complexes $[Ru(\eta^5\text{-}C_5H_5)(PPh_3)_2(=C=CH\{R\})][OTf]$ (R = Ur, **3a**[OTf]; R = Ph, **3b**[OTf]; R = C_6H_4-3-OMe, **3c**[OTf]) with ten equivalents of PPh_3 in CH_2Cl_2 at reflux resulted in the formation of the corresponding vinyl complexes $[Ru(E\text{-}CH=C\{PPh_3\}R)(\eta^5\text{-}C_5H_5)(PPh_3)_2][OTf]$, **6a–c**[OTf], in excellent yield (Scheme 1). The structure of these species was determined by NMR spectroscopy, elemental analysis and single crystal X-ray diffraction. As demonstrated by X-ray crystallography, complexes **6a–c**[OTf] (Fig. 4, 5, 6) form an isostructural series with a similar series of bond lengths and angles. Indeed, the metrical parameters for the alkenyl-phosphonio ligand within these species and those previously reported in the literature (Table 5) are closely related, although the M–C_a bond lengths within the Cp-ligated complexes reported in this study do appear to be somewhat longer that the related *p*-cymene and indenyl-substituted species. Within this series of complexes the most marked structural difference is in the orientation of the $[Ru(\eta^5\text{-}Ind')(EE\text{-}CH=C\{PPh_3\}Ph)(CO)(PPh_3)]^+$ the alkenyl-phosphonio ligand is essentially parallel to the indenyl ring, whereas in **6a**$^+$ it is perpendicular. The electronic effects which govern the orientation of alkenyl ligands within organometallic complexes have been extensivily studied[17–19] and demonstrate a preference for

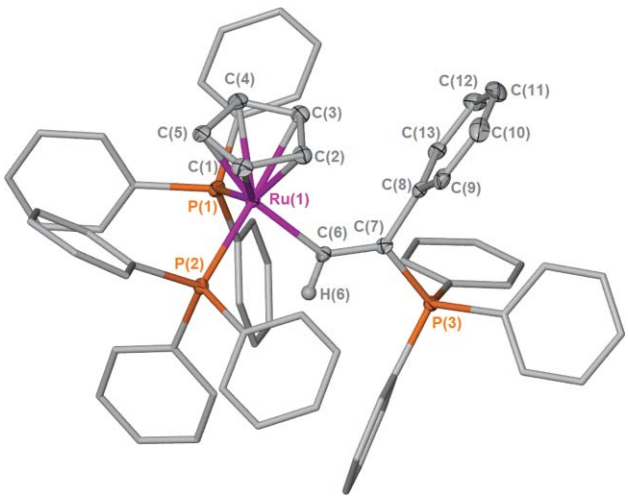

Fig. 5 Structure of the cation of **6b**[OTf]. Selected thermal ellipsoids shown at the 50% probability level. Hydrogen atoms, except H(6), omitted for clarity.

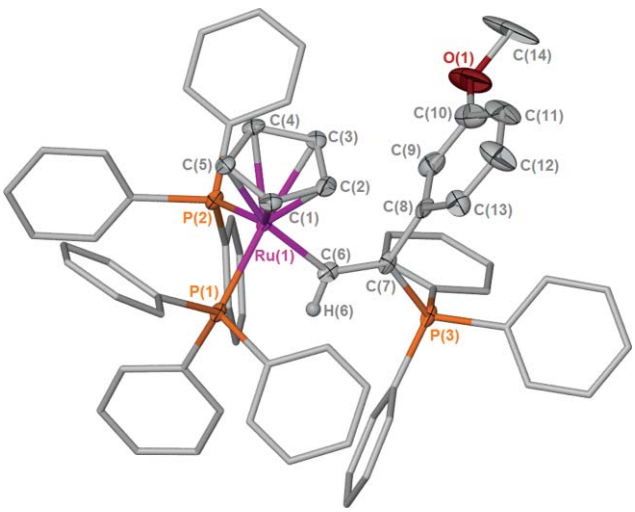

Fig. 6 Structure of the cation of **6c**[OTf]. Selected thermal ellipsoids shown at the 50% probability level. Hydrogen atoms, except H(6), omitted for clarity. The OMe group is disordered over two positions.

Table 5 Comparison of bond lengths (Å) and angles (°) in alkenyl-phosphonio complexes[a]

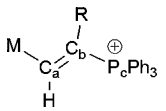

Complex	M–C_a	C_a–C_b	C_b–P_c	M–C_a–C_b	C_a–C_b–P_c	C_a–C_b-R	R–C_b–P_c	*Cen*–M–C_a–C_b	Ref.
$[Ru(\eta^5\text{-}C_9H_7)(E\text{-}CH{=}C\{PPh_3\}\{C{=}CH\textit{cyhex}\})(PPh_3)_2]^+$	2.045(6)	1.371(7)	1.790(6)	135.9(4)	117.5(4)	129.6(5)	112.5(4)	4.5	14
$[Ru(\eta^5\text{-}C_9H_7)(E\text{-}CH{=}C\{PPh_3\}CH{=}CHFc)(PPh_3)_2]^+$	2.039(8)	1.354(11)	1.783(8)	133.5(7)	120.4(6)	125.2(7)	114.4(6)	40.8	15
$[Ru(\eta^5\text{-}Ind')(EE\text{-}CH{=}C\{PPh_3\}Ph)(CO)(PPh_3)]^+$	2.039(7)	1.344(10)	1.801(7)	135.6(6)	120.5(6)	124.9(7)	114.5(5)	107.0	15
$[Ru(\eta^6\text{-}p\text{-cymene})(E\text{-}CH{=}C\{PPh_3\}Ph)Cl(PPh_3)]^+$	2.053(3)	1.343(4)	1.801(2)	131.3(2)	115.9(2)	128.5(3)	115.5(2)	58.6	16
$[Ir(\eta^5\text{-}C_5Me_5)(E\text{-}CH{=}C\{PPh_3\}Ph)Cl(PPh_3)]^+$	1.99(2)	1.42(3)	1.80(2)	133(1)	115(1)	129(1)	115(1)	61.1	16
$[Rh(\eta^5\text{-}C_5H_5)(E\text{-}CH{=}C\{PPh_3\}Ph)Cl(PPh_3)]^+$	1.99(2)	1.36(3)	1.84(2)	137(1)	116(1)	127(2)	115(1)	60.2	16
[6a]$^+$	2.063(5)	1.377(6)	1.788(5)	135.0(4)	118.2(4)	128.1(5)	113.7(3)	1.9	[b]
[6b]$^+$	2.090(2)	1.357(3)	1.798(3)	133.59(19)	120.63(19)	128.2(2)	110.96(17)	23.9	[b]
[6c]$^+$	2.070(5)	1.366(7)	1.791(5)	133.6(4)	121.0(4)	128.0(5)	110.7(4)	24.6	[b]

[a] Abbreviations used *cyhex* = cyclohex-1-enyl; *Cen*= centroid of aromatic ligand, Ind′ = 1,2,3-$Me_3C_9H_4$. [b] This work.

orientation in which d–π*-backbonding is maximised. However, given that the stabilisation provided by this interaction is only *ca.* 28 kJ mol^{-1} and in the phosphonio-substituted complexes alkenyl ligands are observed in plane with both π-base and π-acid ligands it is likely that the precise geometry in these complexes is dictated by steric effects, given the bulky groups present.

The ^{1}H NMR spectrum of **6b**[OTf] exhibited a downfield resonance at δ 10.71 (dt, $^3J_{PP}$ = 36.9 Hz, $^3J_{PP}$ = 9.2 Hz), in conjunction with a resonance at δ 204.4 (dt, $^2J_{PC}$ = 16.1 Hz, $^2J_{PC}$ = 6.4 Hz) in the ^{13}C{^{1}H} NMR spectrum confirming the presence of the alkenyl ligand: similar resonances were observed in the case of **6a**[OTf] and **6c**[OTf]. The positioning of the PPh_3 groups within **6b**[OTf] was demonstrated in the ^{31}P{^{1}H} spectrum by a doublet resonance at δ 47.68 (d, $^4J_{PP}$ = 5.7 Hz) for the Ru-bound PPh_3 ligands with a corresponding triplet for the PPh_3 bonded to the alkenyl ligand at δ 17.46 (t, $^4J_{PP}$ = 5.7 Hz): the appearance of this spectrum did not alter with temperature. The ^{31}P{^{1}H} NMR spectra of **6a**[OTf] and **6c**[OTf] were somewhat more complex. In the case of **6a**[OTf] the ^{31}P{^{1}H} NMR spectrum in CD_2Cl_2 exhibited a resonance at δ 16.1 (t, $^4J_{PP}$ = 5.6 Hz) for the PPh_3 group coordinated to the alkenyl group, and two further peaks for the PPh_3 groups coordinated to the ruthenium were observed as an AB pattern at δ 46.8 (dd, $^2J_{PP}$ = 35.2 Hz, $^4J_{PP}$ = 5.6 Hz) and δ 46.3 (dd, $^2J_{PP}$ = 35.2 Hz, $^4J_{PP}$ = 5.6 Hz). The appearance of these later resonances altered markedly with temperature (Fig. 7). Similar behaviour was observed for **6c**[OTf]: at 300 K a resonance at δ 17.3 (apparent triplet,$^4J_{PP}$ = 5.6 Hz) for the PPh_3 bonded to the alkenyl group was observed: two further peaks, for the PPh_3 ligands coordinated to the ruthenium, were observed as an AB pattern at δ 47.68 (apparent d, 5.6 Hz) and δ 47.67 (apparent d, 5.6 Hz). On cooling the solution to 235 K the AB pattern becomes an apparent triplet at δ 47.84. At 195 K the spectrum appears as would be expected on the basis of the crystal structure: the upfield resonance at δ = 17.8 remains a triplet ($^4J_{PP}$ = 5.5 Hz) but the downfield resonance can be seen as two separate doublet of doublets at δ = 48.26 ($^2J_{PP}$ = 35.0 Hz, $^4J_{PP}$ = 5.4 Hz) and δ = 48.02 ($^2J_{PP}$ = 35.0 Hz, $^4J_{PP}$ = 5.4 Hz). Simulations of the spectra† reveal that the changes in lineshape of the resonances may be modeled by changes of chemical shift of these two resonances with temperature, rather than the effects of a dynamic process.

Clearly the mirror plane which exists in **6b**[OTf] is not present in **6a**[OTf] or **6c**[OTf] due to the presence of the unsymmetrical substituent (Ur, or C_6H_4-3-OMe) on the alkenyl ligand. Any rotation of this group must be slow on the NMR timescale ensuring that the two ruthenium-bound PPh_3 ligands remain inequivalent.

The aromatic region of the ^{1}H NMR spectra for **6a–c**[OTf] also showed significant and essentially identical temperature dependence. In the case of **6b**[OTf] three broad resonances between δ = 7.37 and δ = 6.99 were observed: these peaks overlapped with other, sharp, resonances in the phenyl region. Cooling the sample to 195 K led to these broad peaks sharpening significantly, with six new resonances observed at δ = 7.62, 7.50, 7.28, 6.85, 6.47 and 6.25. This observation is consistent with the phenyl groups in the two ruthenium-coordinated phosphines becoming inequivalent. This assignment was supported by a series of selectively decoupled ^{1}H{^{31}P} NMR experiments (700 MHz, 260 K).

The broad nature of the phenyl resonances from the ruthenium-bound phosphines at 300 K indicates that rotation around the Ru–P bond is becoming slow on the NMR timescale. Presumably phosphine rotation is being hindered by a steric interaction. A ^{1}H-^{1}H NOESY experiment revealed a strong nOe interaction between the proton in the α-position of the alkenyl ligand and the protons on the phenyl rings of the ruthenium-coordinated triphenylphosphine. Examination of the crystal structures of **6a–c**[OTf] reveals that this hydrogen sits in a "pocket" between the two phosphine ligands. The NMR spectra demonstrate that this is also the case in solution, with the hydrogen atom being forced down into the pocket and presumably hindering phosphine rotation.

The poor solubility of **6a**[OTf] in CD_2Cl_2 precluded us from studying the concentration dependence of the NMR spectra of this species. Although the complex was more soluble in d_4-MeOD, facile H/D exchange in this solvent meant the N–H resonances were not observable. However, the N–H region of the ^{1}H NMR spectrum of **6a**[OTf]–in common with that of **5a**[OTf], displays significant temperature dependence, with both N–H resonances moving downfield as the temperature is decreased (Fig. 8). In this case, the N–H(3) proton show smaller changes in chemical shift than N–H(1) which is consistent with aggregation processes occurring in solution principally *via* motifs **D**–**E** (Fig. 1).

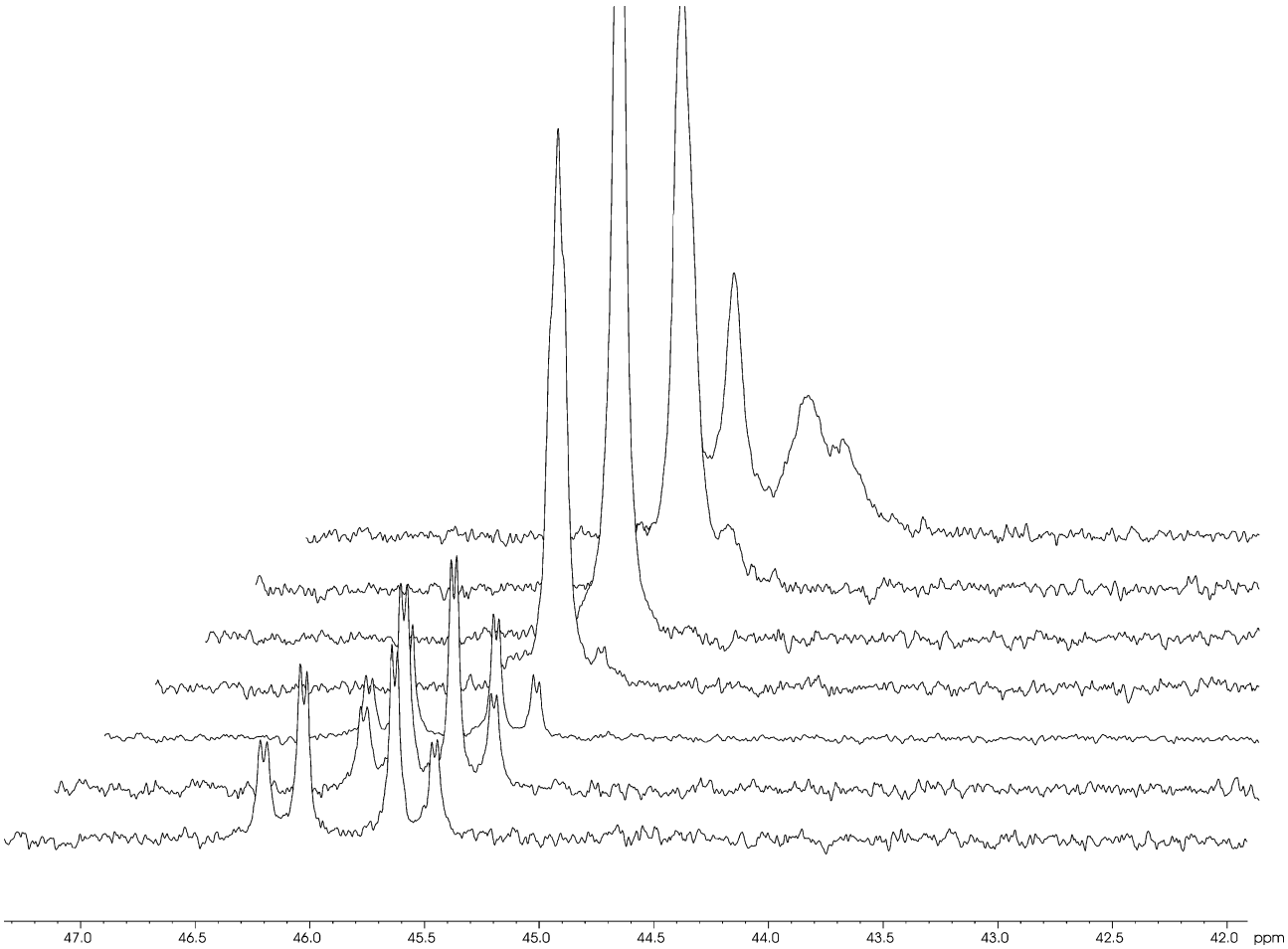

Fig. 7 Variable temperature $^{31}P\{1H\}$ NMR spectrum of **6a**[OTf] in CD_2Cl_2 solution. Only the resonances for the ruthenium-bound PPh_3 ligands are displayed. Spectra recorded at 20 K intervals with the foremost spectrum at 300 K, and the rearmost at 220 K.

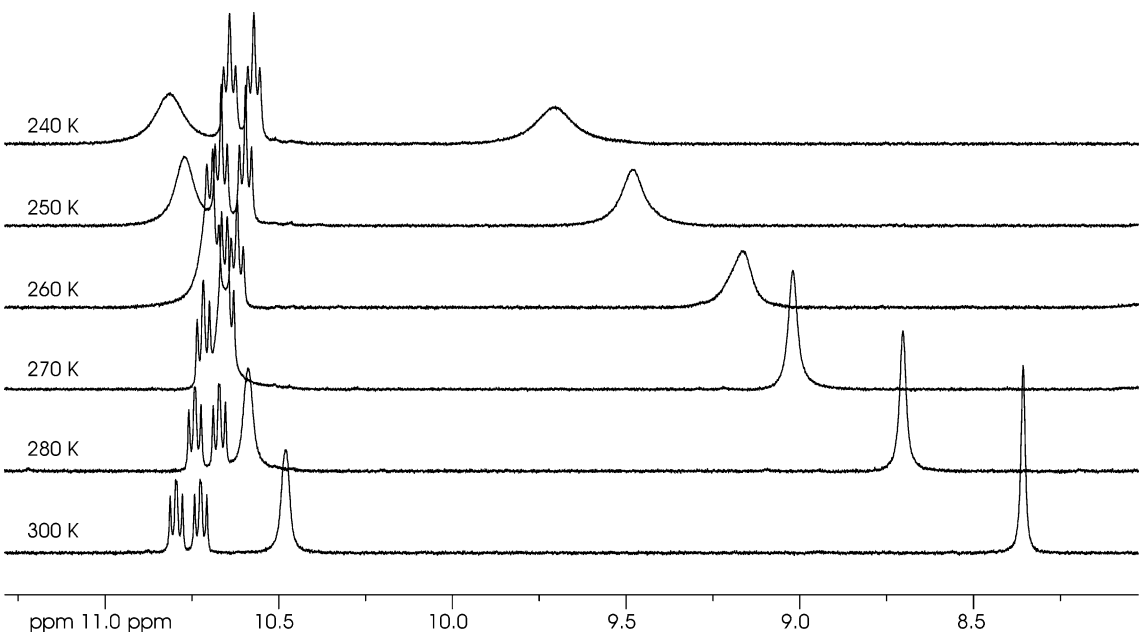

Fig. 8 The N–H region of the ^1H NMR spectrum of **6a**[OTf] in CD_2Cl_2 solution recorded at various temperatures.

Mechanism of formation of β-alkenyl phosphonio salts. Intermolecular nucleophilic addition of PPh_3 to the α-carbon of vinylidene ligands has been proposed in the formation of $[Fe(C\{PPh_3\}{=}CH_2)(\eta^5\text{-}C_5H_5)(CO)(PPh_3)]^+$,[20] and in the reaction of $[Ru(\eta^5\text{-}C_5R_5)(PPh_3)_2(=C{=}CH_2)]^+$ (R = H, Me) with tertiary phosphines.[21] However, this does not appear to be a viable pathway for the formation of the salts of **6**$^+$ from **3**$^+$ as, for example, there is no obvious mechanism for how this would explain the observed stereochemistry in the product.

A more plausible mechanism for the formation of **6**$^+$ is shown in Scheme 2. The vinylidene **3**$^+$ is proposed to be in equilibrium with the η^2(2e)-alkyne complex **7**$^+$. Nucleophilic attack by PPh_3 onto the substituted carbon atom provides a simple rationale for the formation of **6**$^+$. It is proposed that attack at the α-carbon is prohibited for steric reasons as in the examples above where such a reaction pathway is observed the vinylidene ligand is unsubstituted. Presumably the reaction is under thermodynamic control as the nucleophilic attack at the other alkyne carbon atom will place the more bulky aryl group α to the metal, which is anticipated to be less favoured: a kinetic preference for the formation of **6**$^+$ based on electronic arguments cannot be discounted.

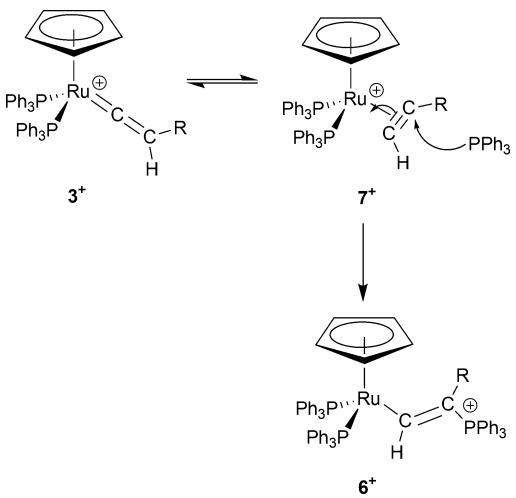

Scheme 2 Mechanism of formation of **6**$^+$.

Although Gimeno *et al.* have demonstrated that the alkyne-form of related half-sandwich ruthenium complexes may be observed with the correct combination of ligands and indeed reacts with PPh_3 to give alkenyl-phosphoino complexes,[15] this is, to the best of our knowledge, the first experimental evidence for the presence of **7**$^+$ in solutions of the vinylidene complex, **3**$^+$.

In an attempt to obtain further evidence for a significant equilibrium between **3**$^+$ and **7**$^+$ a CD_2Cl_2 solution of **3b**[PF_6] was treated with an excess of PhC≡^{13}CH. We reasoned that if **7**$^+$ was present in solution it might be possible to exchange the η^2-coordinated alkyne, furthermore the use of the labelled phenylacetylene would ensure that the process was essentially degenerate (Scheme 3). Exchange of free and coordinated alkyne does indeed take place: in the $^{31}P\{^1H\}$ NMR spectrum a new doublet resonance (δ 42.68, $^2J_{PC}$ = 15.4 Hz) is observed to grow, whilst in the ^{1}H NMR spectrum the doublet resonance for the alkyne proton of PhC≡^{13}CH decreases in intensity and a singlet for PhC≡CH

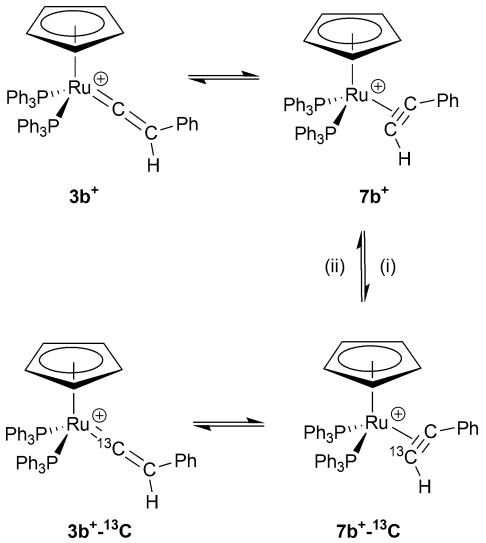

Scheme 3 Exchange of coordinated alkyne ligands (i) + PhC≡^{13}CH, – PhC≡CH; + PhC≡CH, – PhC≡^{13}CH.

was observed. These results are consistent with the formation of $[Ru(\eta^5\text{-}C_5H_5)(PPh_3)_2(^{13}C{=}CHPh)]^+$, **3b**$^+$-^{13}C and after 5 days, approximately 46% of the vinylidene complex possessed a ^{13}C-label. These results therefore provide further circumstantial evidence for the presence of **7**$^+$ in equilibrium with **3**$^+$. A mechanism for the alkyne/vinylidene exchange based on loss of a phosphine ligand from **3b**$^+$ may also be possible. In this case a putative intermediate $[Ru(\eta^5\text{-}C_5H_5)(\eta^2\text{-}H^{13}C{\equiv}CPh)(C{=}C\{Ph\}H)(PPh_3)]^+$ may be proposed that could allow for the incorporation of the ^{13}C label. However, under the conditions employed no evidence for the formation of dimers of the alkyne was obtained which might be expected if this were indeed the case.

Further reactions of 6b[OTf] and 6c[OTf]. After leaving a CD_2Cl_2 solutions of **6c**[OTf] to stand at room temperature for approximately five weeks, it was observed that the solution had undergone a colour change from bright yellow to deep red. ^{1}H and $^{31}P\{^1H\}$ NMR spectroscopy revealed that 60% of the **6c**[OTf] present in the original sample had been converted into a new product, **8c**[OTf]. Complex **8c**[OTf] could be conveniently prepared by heating a $C_2H_2Cl_4$ solution of **6c**[OTf] at 100 °C for 1 h. Although we have not been able to unambiguously determine the structure of **8c**[OTf] by a single crystal X-ray diffraction study, the complex was characterised by a combination of NMR spectroscopy and mass spectrometry. The ^{1}H NMR spectrum of **8c**[OTf] exhibited a resonance at δ 4.77 for a cyclopentadienyl ligand and, in addition to a series of resonances in the aromatic region, two distinctive multiplets at δ 4.61 (ddd, $^3J_{PaH}$ = 22.0, $^2J_{HH}$ = 3.8, $^3J_{PbH}$ = 1.5 Hz) and 2.17 (ddd, $^3J_{PaH}$ = 22.1, $^3J_{PbH}$ = 18.2, $^3J_{HH}$ = 3.8 Hz), integrating to one proton each, relative to the cyclopentadienyl resonance. The nature of the couplings were assigned on the basis of selective and broad-band $^1H\{^{31}P\}$ NMR experiments. The $^{31}P\{^1H\}$ NMR revealed two resonances, mutually coupled doublets at δ 52.38 (d, J_{PP} = 3.5 Hz, P_a) and 46.92 (d, J_{PP} = 3.5 Hz, P_b). The small size of the coupling constant between the two phosphorus atoms strongly suggested that the compound did not retain the two *cis* phosphine ligands of **6c**[OTf]. These data also indicated that a PPh_3 group had been lost in the

formation of **8c**[OTf]. A ^{1}H-^{13}C HMQC experiment revealed a resonance at δ 43.51 (t, $J = 8.2$ Hz) correlated to the two multiplets seen at δ 4.61 and 2.17 in the ^{1}H NMR spectrum. A DEPT-135 experiment confirmed that this resonance was due to a CH_2 group. Complex **6b**[OTf] underwent a related reaction to give a product **8b**[OTf] which exhibited a similar series of resonance in its NMR spectra to **8c**[OTf], although prolonged heating resulted in decomposition in this case.

The ESI mass spectrum of **8c**[OTf] contained two major peaks: the first at *m/z* 823.1843 was assigned to the molecular ion **8c**$^{+}$, confirming the loss of a PPh_3 group from **6c**$^{+}$ and, critically, a peak at *m/z* 395, assigned to $[(C_6H_4\text{-}3\text{-}OMe)(PPh_3)C{=}CH_2]^{+}$.

Two structures (**G** and **H**, Scheme 4) which vary in which PPh_3 group has undergone the cyclometallation reaction were considered for **8**$^{+}$. Compound **G** (in which R = H) has been prepared by Onitsuka and co-workers from the reaction between $[Ru(\eta^5\text{-}C_5H_5)(=C{=}CH_2)(PPh_3)_2]^{+}$ with PPh_3.[21] The ^{1}H and ^{31}P{^{1}H} NMR data of **8**$^{+}$ and the compounds with structure **G** are closely related. However, our observation of $[(C_6H_4\text{-}3\text{-}OMe)(PPh_3)C{=}CH_2]^{+}$ in the mass spectrum suggest structure **H** for **8**$^{+}$. In addition, the formation of the CH_2 group in **8c**[OTf] is contradictory to the elegant deuterium labelling experiments performed by Onitsuka *et al.*, which would suggest that, if structure **G** had been formed, the PPh_3 group in the alkene ligand should be geminal to one of the two protons: this is clearly not the case in **8c**$^{+}$. The difference in behaviour may be explained by the different sites of nucleophilic attack in the substituted and un-substituted vinylidene complexes. In the case of the un-substituted species, Onitsuka *et al.* obtained evidence for nucleophilic attack by both PPh_3 and PMe_2Ph at the α-carbon of the vinylidene ligand. In the case of our aryl-substituted complexes we believe that this pathway is inhibited for steric reasons and thus favour structure **H**.

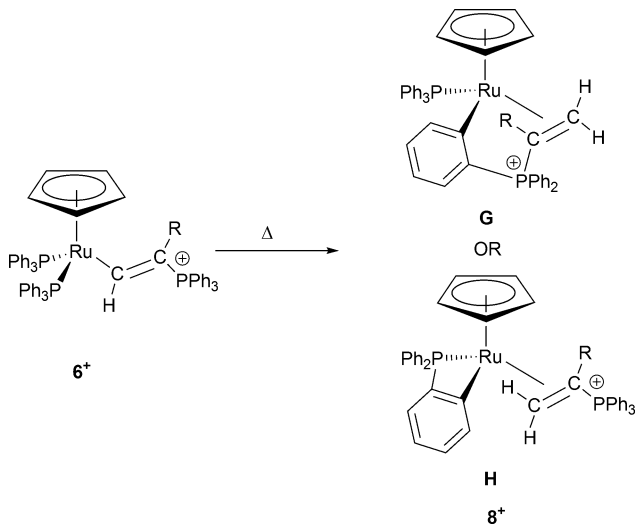

Scheme 4 Possible structures for **8**$^{+}$.

Mechanistic study into the formation of 8b[OTf]. Monitoring the reaction of **6b**[OTf] in CD_3CN solution gave insight into the mechanism by which **8b**[OTf] was formed. This study revealed that even at room temperature, loss of a PPh_3 ligand from the ruthenium was occurring. In the ^{1}H NMR spectrum, the resonance for the proton attached to the α-carbon of the alkenyl ligand of **6b**[OTf] was observed at δ 10.75 (dt, $^{3}J_{HP} = 37.1$ Hz, $^{3}J_{HP} = 9.1$ Hz) as well as a resonance for a new species, **9b**[OTf] at δ 10.61 (dd, $^{3}J_{HP} = 34.7$ Hz, $^{3}J_{HP} = 11.3$ Hz). A resonance for the cyclopentadienyl ligand in **9b**[OTf] was observed at δ 4.23. The ^{31}P{^{1}H} NMR revealed, in addition to the resonances for **6b**[OTf], two new resonances at δ 61.01 (d, $^{4}J_{PP} = 6.3$ Hz) and δ 14.43 (d, $^{4}J_{PP} = 6.3$ Hz). These data indicated that **9b**[OTf] has been formed by phosphine loss from **6b**[OTf] and, as such, **9b**[OTf] is assigned the formula $[Ru(E\text{-}CH{=}C\{PPh_3\}Ph)(\eta^5\text{-}C_5H_5)(NCMe)(PPh_3)][OTf]$. The ratio of **9b**[OTf] to **6b**[OTf] was 1 : 5, however, on heating the sample at 60 °C for 4 h, the relative amount of **9b**[OTf] decreased (ratio **9b**[OTf] : **6b**[OTf] 1 : 33) and resonances for **8b**[OTf] were now observed, which corresponded to approximately 4% conversion. After heating the sample for a further six days, the yield of **8b**[OTf] had increased to approximately 20%. The quantity of **9b**[OTf] relative to **6b**[OTf] had decreased still further: they were now present in a 1 : 45 ratio. In addition a further doublet resonance was observed at δ 9.01 (d, $^{3}J_{HP} = 28.8$ Hz) which was assigned to $[Ru(E\text{-}CH{=}C\{PPh_3\}Ph)(\eta^5\text{-}C_5H_5)(NCMe)_2][OTf]$, **10b**[OTf].

The rapid initial consumption of **9b**[OTf] upon heating of the solution indicates that it may be an intermediate along the path to form the phosphonio-alkene complex **8b**[OTf]. Furthermore, because **9b**[OTf] remains at a low concentration relative to the starting material once the solution is heated and formation of **8b**[OTf] begins, it would seem that loss of phosphine from **6**[OTf] is the rate determining step in the reaction to form **8**[OTf].

These results are directly relevant to the formation **8b**[OTf] and **8c**[OTf] in CD_2Cl_2 and tetrachloroethane. When a sample of **6c**[OTf] in CD_2Cl_2 solution was allowed to stand at room temperature for several days, ^{1}H NMR spectroscopy revealed resonances similar to those observed for **9b**[OTf] in acetonitrile, for the product of phosphine loss.

The following mechanism for the formation for the cations **8**$^{+}$ (with structure **H**) is proposed (Scheme 5). Initial loss of a phosphine ligand from **6**$^{+}$ results in the formation of vacant coordination site at the metal to give **I**. This species may then react with NCMe to give **9**$^{+}$ and subsequently **10**$^{+}$ or an *ortho*-metallation reaction may occur to give a hydride-containing intermediate **J**. Subsequent reduction elimination of the phosphonio-substituted alkene may then occur to give **8**$^{+}$. Related *ortho*-metallation reactions have been observed by Bruce and co-workers in the $Ru(\eta^5\text{-}C_5H_5)Me(PPh_3)_2$ system.[22]

Conclusions

It is somewhat remarkable that the synthetic chemistry employed to prepare the uracil-containing complexes is essentially identical to that when more simple aromatic groups are present. Indeed, the only significant difference in behaviour that is observed appears to be that the nucleobase-containing species are far less soluble, an observation which we rationalise in terms of enhanced aggregation effects. These results indicate that even in the presence of the functionalised uracil substituent the core chemistry of the cyclopentadienyl ruthenium fragment remains unchanged.

The solid state structure of both **5a**[OTf], **5a**[PF_6] and **6a**[OTf] all exhibit the same hydrogen bonding motif, *viz* a symmetric dimer employing N–H(3) and C=O(4): N–H(1) engages in hydrogen bonding to the anion. The same pattern is observed in

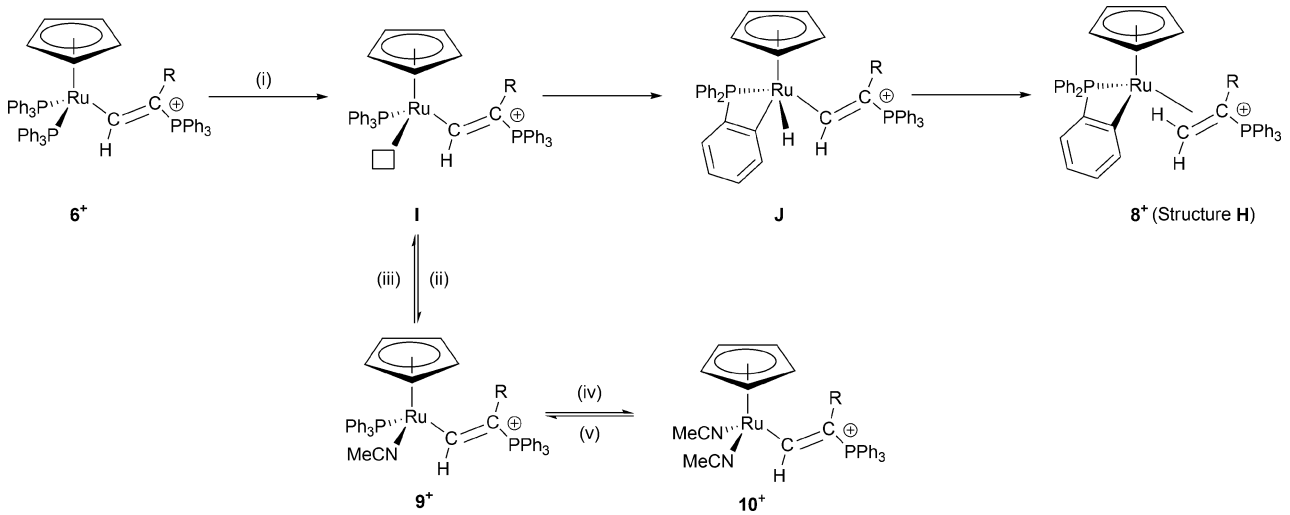

Scheme 5 (i) – PPh_3; (ii) + NCMe; (iii) – NCMe; (iv) – PPh_3, + NCMe; (v) + PPh_3, – NCMe.

[Mo(=C=CHUr)(η^7-C_7H_7)(dppe)][BF_4]. This is in contrast to the solid state structure of the cations of **3**$^+$ which forms a hexagonal rosette. The origin of the differences in structure may be traced back the geometries of the individual cations involved. In **3a**$^+$, the uracil and cyclopentadienyl ligand are almost co-planar and the nucleobase is also remote from the other ligands of the complex. In contrast in **5a**[OTf], **5a**[PF_6] and **6a**[OTf] and the molybdenum complex, the uracil group is perpendicular to the π-ligand ensuring that the uracil is more crowded by the PPh_3 or dppe ligands hence restricting the aggregation in the solid state.

A similar argument provides a convenient explanation for the pronounced aggregation effects observed in **4a** when compared to the carbene and β-alkenyl-phosphoino complexes. In the structure of **4a** the uracil group will be remote from the PPh_3 ligands and hence there will be fewer steric constraints on the formation of the aggregates. A complementary explanation for the enhanced aggregation is that **4a** is neutral and as such it would be expected that any Columbic repulsions present in, for example, **3a**$^+$ and **5a**$^+$ would not be present.

We have also developed a convenient route to the synthesis of cyclopentadientyl-substituted β-alkenyl phosphonio complexes of type **6**$^+$. It appears that this reaction proceeds *via* the less favourable alkyne isomer of the vinylidene complex and that phosphine loss from these species is facile, possibly due to the presence of three PPh_3 groups in close proximity.

Experimental

All experimental procedures were performed under an atmosphere of dinitrogen or argon using standard Schlenk line and glove box techniques. Solvents were purified by distillation under argon prior to use from appropriate drying agents (MeOH from Mg/I_2; CH_3CN and CH_2Cl_2 from CaH_2; Et_2O from Na wire; acetone from Drierite). The CD_2Cl_2 used for NMR experiments was dried over CaH_2 and degassed with three freeze-pump-thaw cycles. The compounds RuCl(η^5-C_5H_5)(PPh_3)$_2$, **1**,[23] HC≡CUr, **2**,[24] and [Ru(η^5-C_5H_5)(PPh_3)$_2$(=C=CHUr)][OTf], **3a**[OTf],[8] [Ru(η^5-C_5H_5)(PPh_3)$_2$(=C=CHPh)(PPh_3)$_2$][OTf], **3b**[OTf],[9] were prepared according to published procedures.

NMR spectra were acquired on a Bruker AV 500 spectrometer (operating frequencies ^{1}H 500.13 MHz, ^{31}P 202.47 MHz, ^{13}C 125.77 MHz) or a Bruker Avance 700 Spectrometer (operating frequencies ^{1}H 700.13 MHz, ^{31}P 283.46 MHz). Solution NMR studies were performed using standard CD_2Cl_2 solutions of **4a** made to the appropriate concentrations by using serial dilution. Simulations of NMR spectra were performed with the gNMR suite of programmes.[25] IR spectra were acquired using a Mattson Research Series FTIR spectrometer as a KBr disk. Mass spectrometry measurements were performed on Fisons Analytical (VG) Autospec (Fast Atom Bombardment) and Thermo-Electron Corp LCQ Classic (ESI) instruments.

Synthesis of [Ru(η^5-C_5H_5)(PPh_3)$_2$(=C=CH-{C_6H_4-3-OMe})][OTf], 3c[OTf]

RuCl(η^5-C_5H_5)(PPh_3)$_2$ (489 mg, 0.67 mmol) and NH_4OTf (225 mg, 1.34 mmol) were placed in a Schlenk tube and suspended in methanol (20 mL). 3-Methoxyphenylacetylene (178 mg, 205 μl, 1.34 mmol) was added to the solution, which was heated at reflux for 10 min (until turning deep red). The solvent was removed *in vacuo* and the red solid extracted with dichloromethane (2 × 10 mL). The extracts were reduced in volume to 10 mL and triturated with ether to give a red powder, which was isolated by filtration. The red solid was washed with ether (3 × 10 mL). Yield 589 mg, 90%. The structure of **3c**[OTf] was also confirmed by single crystal X-ray diffraction: see ESI.† ^{1}H NMR: (CD_2Cl_2, 300 K) δ = 7.42 (m, 6H, P*Ph*$_3$), 7.24 (m, 12H, P*Ph*$_3$), 7.19 (t, 1H C_6H_4-3-OMe), 7.05 (m, 12H P*Ph*$_3$), 6.69 (m, 2H, C_6H_4-3-OMe), 6.62 (m, 1H, C_6H_4-3-OMe), 5.41 (t, $^4J_{HP}$ = 2.5 Hz, 1H, =C=C(*H*) C_6H_4-3-OMe), 5.27 (s, 5H, C_5H_5), 3.60 (s, 3H, C_6H_4-3-O*Me*). ^{31}P{^{1}H} NMR: (CD_2Cl_2, 300 K) δ = 42.43 (s, *P*Ph_3). ^{13}C{^{1}H} NMR: (CD_2Cl_2, 300 K) δ = 353.85 (t, $^2J_{PC}$ = 15.4 Hz, Ru=*C*), 160.02 (s, *C*-OMe), 133.57 (dd, $^1J_{PC}$ = 51.7 Hz, $^3J_{PC}$ = 9.6 Hz, PPh_3 C-1), 133.56, 133.13, 131.15, 129.93, 128.73, 128.61 (multiplets, *Ph*), 121.14 (q, $^1J_{CF}$ = 321.4 Hz *C*F_3), 119.66, 119.55 (multiplets, *Ph*), 112.72 (d, $^3J_{PC}$ = 32.3 Hz C-β), 95.05 (s, C_5H_5), 55.14 (s, O*C*H_3). FAB mass spectrum: m/z = 823 [M$^+$], m/z = 691 [M$^+$ - $HC_2C_6H_4$-3-OMe], m/z = 561 [M$^+$ - PPh_3], m/z = 429

[M^+ - PPh_3, $HC_2C_6H_4$-3-OMe]. Elemental Analysis: Expected for $C_{69}H_{58}F_3O_4P_3RuS$: C 67.15% H 4.74%; Found: C 66.94% H 4.82%.

Synthesis of Ru(-C≡CUr)(η⁵-C_5H_5)(PPh_3)$_2$, 4a

$RuCl(\eta^5\text{-}C_5H_5)(PPh_3)_2$ (500 mg, 0.68 mmol), ethynyluracil (185 mg, 1.35 mmol) and NH_4PF_6 (230 mg, 1.41 mmol) were suspended in methanol (30 mL) and heated (with stirring) at 60 °C for 2 h, after which time the solution had turned a deep red colour. The solution was filtered and 1 M NaOMe in MeOH (0.7 mL) was added. The solution underwent an immediate colour change from red to bright yellow. Addition of hexane to the solution resulted in the formation of a yellow microcrystalline solid which was isolated by filtration. ^{1}H NMR (d_6-DMSO, 6.0 mM) $\delta = 4.12$ (s, C_5H_5); ^{31}P NMR (d_6-DMSO, 6.0 mM) $\delta = 49.44$ (s, PPh_3). Mass spectrum: $m/z = 849$ [Ru(C≡CUr)(η⁵-C_5H_5)(PPh_3)$_2$]+Na^+, $m/z = 826$ [Ru(C≡CUr)(η⁵-C_5H_5)(PPh_3)$_2$]$^+$, $m/z = 719$ [Ru(η⁵-C_5H_5)(PPh_3)$_2$CO]$^+$, $m/z = 691$ [Ru(η⁵-C_5H_5)(PPh_3)$_2$]$^+$, $m/z = 429$ [Ru(η⁵-C_5H_5)(PPh_3)]$^+$. IR: (CH_2Cl_2 cm^{-1}) 3435 (br, N–H), 2073 (m, C≡C), 1618 (br, C=O).

Synthesis of [Ru(η⁵-C_5H_5)(PPh_3)$_2${=C(OMe)-CH_2Ur}][OTf], 5a[OTf]

$RuCl(\eta^5\text{-}C_5H_5)(PPh_3)_2$ (250 mg, 0.34 mmol), ethynyluracil (90 mg, 0.66 mmol) and NH_4OTf (55 mg, 0.33 mmol) were suspended in methanol (30 mL) and heated, with stirring, at reflux for 16 h. During this time the colour of the solution changed from orange to yellow. After cooling to room temperature the solution was filtered and the volume of the filtrate reduced until precipitation began to occur. Toluene (2 mL) was added to the solution. On standing, yellow crystals formed. Yield 232 mg, 68%. ^{1}H NMR: ($CDCl_3$) $\delta = 10.05$ (s, 1H, N*H*), 8.62 (s, 1H, N*H*), 7.46 (t, $J = 7.5$ Hz, 6H Ph), 7.33 (t, $J = 7.5$ Hz, 12H Ph), 7.17 (s, 1H, Uracil C*H*), 7.01 (t, $J = 8.4$ Hz, 12H, Ph), 4.91 (s, 5H, C_5H_5), 4.30 (s, 2H, CH_2), 3.38 (s, 3H, OCH_3). ^{31}P{^{1}H} NMR: ($CDCl_3$) $\delta = 45.32$ (s, PPh_3) ^{13}C{^{1}H} NMR: ($CDCl_3$): $\delta = 305.4$ (t, $^2J_{PC} = 12.1$ Hz, Ru=C), 163.66 (s, CO), 150.03 (s, CO), 142.64 (s, H*C*=C), 137.91 (s, HC=*C*), 135.71 (d, $J = 45.4$ Hz PPh_3, C_1), 133.45 (vt, $|^2J_{PC}+{}^4J_{PC}| = 5.1$ Hz, PPh_3, C_2), 132.16 (d, $J = 9.9$ Hz, PPh_3, C_3), 131.99 (d, $J = 3.0$ Hz, PPh_3, C_4), 91.54 (s, C_5H_5), 63.61 (s, OCH_3), 30.97 (s, CH_2).

Synthesis of [Ru(*E*-CH=C{PPh_3}Ur)(η⁵-C_5H_5)(PPh_3)$_2$][OTf], 6a[OTf]

$RuCl(\eta^5\text{-}C_5H_5)(PPh_3)_2$ (500 mg, 0.68 mmol) and NH_4OTf (126 mg, 0.74 mmol) were suspended in methanol (30 mL). Ethynyl-uracil (185 mg, 1.36 mmol) was added to the reaction mixture, which was heated at reflux for 2 h, during which time the solution became red. Upon cooling, the reaction mixture was filtered and the solvent removed *in vacuo*. The red solid so obtained was extracted with dichloromethane (3 × 20 mL). The combined extracts were heated at reflux with PPh_3 (1.64 g, 6.80 mmol) for 72 h. After cooling to room temperature, the yellow solution was reduced to dryness and the solid residue washed with toluene (2 × 10 mL). The yellow solid was dissolved in dichloromethane and layered with hexane to give bright yellow crystals. Yield 484 mg, 73%. ^{1}H NMR (CD_2Cl_2) $\delta =$ 10.75 (ddd, $^3J_{HP} = 35.2$ Hz, $^3J_{HP} = 9.5$ Hz, $^3J_{HP} = 7.8$ 1H, Ru-CH), $\delta = 10.48$, (s, br, NH), $\delta = 8.35$ (s, br, NH), $\delta = 7.15$ (46H, Ph, Uracil CH), $\delta = 4.31$ (s, 5H, C_5H_5). ^{31}P NMR (CD_2Cl_2, 300 K) $\delta = 46.11$ (dd, $^2J_{PP} = 35.1$ Hz, $^4J_{PP} = 5.9$ Hz, $RuPPh_3$), $\delta = 45.54$ (dd, $^2J_{PP} = 35.1$ Hz, $^4J_{PP} = 5.0$ Hz, $RuPPh_3$), $\delta = 15.28$ (t, $^4J_{PP} =$ 5.6 Hz); ^{13}C{^{1}H} NMR (CD_3CN, 300 K): $\delta = 211.56$ (t, $^3J_{PC} =$ 16.4 Hz Ru–C), δ 165.59 (s, C=O), δ 151.16 (s, C=O), δ 142.75 (d, $^3J_{PC}$ 5.0 Hz, Uracil C_6), 138.2 (br), 134.37, 134.02 (br), 133.41, 133.07, 129.72, 129.56 (br), 129.25, 128.21, 127.92 (multiplets, *Ph*), 122.14 (d, $^1J_{P\text{-}C} = 83.0$ Hz, C-β), 114.40 (d, $^2J_{PC} = 20.0$ Hz, Uracil C_5), 85.71 (s, C_5H_5). FAB mass spectrum: $m/z = 1089$ [M^+], $m/z =$ 827 [M^+ -PPh_3], $m/z = 565$ [M^+ - 2PPh_3], $m/z = 429$ [M^+ - 2PPh_3, HC_2Ur]. Elemental Analysis: Expected for $C_{66}H_{54}F_3N_2O_5P_3RuS$: C 64.02% H 4.40% N 2.26% Found C 62.29% H 4.29% N 2.35%.

Synthesis of [Ru(*E*-CH=C{PPh_3}Ph)(η⁵-C_5H_5)(PPh_3)$_2$][OTf], 6b[OTf]

$RuCl(\eta^5\text{-}C_5H_5)(PPh_3)_2$ (250 mg, 0.34 mmol) and NH_4OTf (63 mg, 0.37 mmol) were suspended in methanol (20 mL). Phenylacetylene (60 μl, 55 mg, 0.34 mmol) was added to the reaction mixture, which was heated at reflux for 10 min (until turning red). Upon cooling, the reaction mixture was filtered and the solvent removed *in vacuo*. The red solid so obtained was extracted with dichloromethane (2 × 10 mL). Addition of ether to the dichloromethane extract resulted in the formation of a pale pink solid that was isolated by filtration. This solid was dissolved in dichloromethane (20 mL) and PPh_3 (0.9 g, 3.44 mmol) was added to the solution, which was then heated at reflux for 72 h. After cooling to room temperature the yellow solution was reduced to dryness and the solid residue washed with toluene (2 × 10 mL). The yellow solid was dissolved in dichloromethane and layered with hexane to give bright yellow crystals. Yield 246 mg, 77%. ^{1}H NMR: (CD_2Cl_2) $\delta = 10.74$ (dt, $^3J_{HP} = 37.0$ Hz, $^3J_{HP} = 9.4$ Hz, 1H, Ru–C*H*=C{Ph}PPh_3), 7.24 (m, 50H, PPh_3, *Ph*), 3.98 (s, 5H, C_5H_5). ^{31}P{^{1}H} NMR: (CD_2Cl_2) $\delta = 47.68$ (d, $^4J_{PP} = 5.8$ Hz), 17.46 (t, $^4J_{PP} = 5.8$ Hz). ^{13}C{^{1}H} NMR: (CD_2Cl_2, 300 K) $\delta = 204.47$ (td, $^2J_{PC} = 15.8$ Hz, 6.8 Hz, Ru–C), 141.53 (d, $^1J_{PC} = 21.1$ Hz, C–P*Ph*$_3$ C_1), 138.03 (s, br, Ru–P*Ph*$_3$ C_1), 134.03, 133.43, 132.98, 129.52, 129.39, 128.98, 128.52, 127.86 (multiplets, *Ph*), 121.13 (q, $^1J_{CF}$ 321.5 Hz CF_3), 121.61 (d, $^1J_{PC} = 84.4$ Hz, C-β), 116.87 (d, $^2J_{PC} = 62.9$ Hz, *Ph* C-β C_1), 85.64 (s, C_5H_5). FAB mass spectrum: $m/z = 1055$ [M^+], $m/z = 793$ [M^+ - PPh_3], $m/z = 531$ [M^+ - 2PPh_3], $m/z = 429$ [M^+ - 2PPh_3, HC_2Ph]. Elemental Analysis: Expected for $C_{68}H_{58}F_3O_3P_3RuS$: C 67.82% H 4.69%; Found: C 67.48% H 4.69%.

Synthesis of [Ru(*E*-CH=C{PPh_3}C_6H_4-3-OMe)(η⁵-C_5H_5)(PPh_3)$_2$][OTf], 6c[OTf]

[Ru(η⁵-C_5H_5)(PPh_3)$_2$(=C=CH{C_6H_4-3-OMe})][OTf] (128 mg, 0.13 mmol) and PPh_3 (345 mg, 1.31 mmol) were placed in a Schlenk tube and dissolved in dichloromethane (20 mL). The solution was heated at reflux for 96 h until it became bright yellow. The solvent was removed *in vacuo* and the yellow solid residue so obtained was washed with toluene (3 × 10 mL). The yellow solid was dissolved in dichloromethane and layered with ether to give bright yellow crystals. Yield 111 mg, 69%. ^{1}H NMR: (CD_2Cl_2) $\delta = 10.71$ (dt, $^3J_{HP} = 36.9$ Hz, $^3J_{HP} = 9.2$ Hz, 1H, Ru–C*H*), 7.23 (50H, P*Ph*$_3$, C_6H_4-3-OMe), 4.06 (s, 5H, C_5H_5), 3.77 (s, 3H, OMe). ^{31}P NMR: (CD_2Cl_2, 300 K) $\delta = 47.67$ (apparent dd, $^4J_{PP} = 1.9$ Hz), 17.33 (t, $^4J_{PP} = 5.6$ Hz); (CD_2Cl_2, 195 K) $\delta = 48.26$ (dd, $^2J_{PP} = 35.0$ Hz, $^4J_{PP} = 5.4$ Hz), 48.02 (dd, $^4J_{PP} = 35.0$ Hz, $^4J_{PP} = 5.4$ Hz), 17.87

(at, $^4J_{PP}$ = 5.5 Hz). $^{13}C\{^1H\}$ NMR: (CD_2Cl_2, 300 K): δ = 204.15 (td, $^2J_{PC}$ = 15.4 Hz, 4.18 Hz, Ru–C), 159.95 (d, $^4J_{PC}$ = 1.6 Hz, *C*OMe), 142.62 (d, $^1J_{PC}$ = 20.6 Hz, CP*Ph*$_3$ C-1), 138.02 (br, Ru–P*Ph*$_3$, C_1), 134.02, 133.44, 129.51, 129.38, 127.84 (multiplets, *Ph*), 130.01, 125.07, 119.26, 113.20 (doublets, C_6H_4-3-OMe), 121.60 (d, $^1J_{PC}$ = 83.6 Hz, C-β), 120.96 (q, $^1J_{CF}$ 323.8 Hz *C*F_3), 116.52 (d, $^2J_{PC}$ = 61.8 Hz, C β-Ph C_1), 85.72 (s, C_5H_5), 55.34 (s, OCH_3). FAB mass spectrum: *m*/*z* = 1085 [M$^+$], *m*/*z* = 823 [M$^+$ - PPh_3], *m*/*z* = 561 [M$^+$ - 2PPh_3], *m*/*z* = 429 [M$^+$ - 2PPh_3, HC_2PhOMe]. Elemental Analysis: Expected for $C_{70}H_{60}Cl_2F_3O_4P_3RuS$: C 63.73%, H 4.58%; Found: C 62.47%, H 4.74%.

Preparation of [Ru(η^5-C_5H_5){η^2-H_2C=CPh(PPh_3)}-($C_6H_4PPh_2$)][OTf], 8b[OTf]

6b[OTf] (*ca.* 20 mg) was placed in an NMR tube and dissolved in $C_2D_2Cl_4$ (0.5 mL). The solution was heated at 363 K for 30 min. **8b**[OTf] was formed in approximately 50% yield (as shown by $^{31}P\{^1H\}$ NMR spectroscopy). It was not possible to isolate this complex however characterisation was performed by NMR spectroscopy. ^1H NMR ($C_2D_2Cl_4$) δ = 4.78 (s, C_5H_5, 5H), 4.64 (ddd, $^3J_{HP}$ = 22.3 Hz, $^2J_{HH}$ = 3.8 Hz, $^3J_{HP}$ = 2.5 Hz), 2.29 (atd, $^3J_{HP}$ = 17.3 Hz, $^2J_{HH}$ = 3.8 Hz). $^{31}P\{^1H\}$ ($C_2D_2Cl_4$, 373 K) δ = 51.48 (d, *J* = 3.2 Hz), 46.97 (d, *J* = 3.2 Hz).

Preparation of [Ru(η^5-C_5H_5){η^2-H_2C=C(C_6H_4-3-OMe)(PPh_3)}-($C_6H_4PPh_2$)][OTf], 8c[OTf]

6c[OTf] (*ca.* 20 mg) was placed in an NMR tube and dissolved in $C_2D_2Cl_4$ (0.5 mL). The solution was heated at 363 K for 30 min. **8c**[OTf] was formed in approximately 50% yield (as shown by $^{31}P\{^1H\}$ NMR spectroscopy). It was not possible to isolate this complex however characterisation was performed by NMR spectroscopy. ^1H NMR ($C_2D_2Cl_4$) δ = 6.57 (m, 3H, C_6H_4-3-OMe), 6.88 (m, 1H, C_6H_4-3-OMe), 4.77 (s, 5H, C_5H_5), 4.61 (ddd, $^3J_{HP}$ = 22.0, $^2J_{HH}$ = 3.8, $^3J_{HP}$ = 1.5 Hz, =CH_2), 3.57 (s. 3H, O*Me*), 2.17 (ddd, $^3J_{HP}$ = 22.1, $^3J_{HP}$ = 18.2, $^2J_{HH}$ = 3.8 Hz), $^{31}P\{^1H\}$ δ = 52.38 (d, $^3J_{PP}$ = 3.5 Hz), 46.92 (d, $^3J_{HP}$ = 3.5 Hz) $^{13}C\{^1H\}$ δ = 173.94 (dd, $^2J_{PC}$ = 32.9 Hz, $^3J_{PC}$ = 17.0 Hz) 158.7 (s, C_6H_4-3-OMe, C_3), 143.7 (d, $^2J_{CP}$ = 6.4 Hz, C_6H_4-3-OMe, C_1), δ 137.36 (d, $^1J_{PC}$ = 114.4 Hz, P*Ph*$_2$, C_1), 132.72 (d, $^1J_{PC}$ 103.4 Hz, P*Ph*$_3$ C_1), 128.8 (s, C_6H_4-3-OMe, C_6), 122.9 (s, C_6H_4-3-OMe, C_4), 116.1 (s, C_6H_4-3-OMe, C_5), 112.8 (s, C_6H_4-3-OMe, C_6), 92.52 (s, C_5H_5), 54.97 (s, O*Me*) 43.51 (at, $^2J_{PC}$ = 8.2 Hz, =CH_2).

Details of X-ray diffraction experiments

Pertinent data concerning the structural determinations reported are collected in Table 2. Diffraction data were collected at 110 K on a Bruker Smart Apex diffractometer with Mo-Kα radiation (λ = 0.71073 Å) using a SMART CCD camera. Diffractometer control, data collection and initial unit cell determination was performed using "SMART" (v5.625 Bruker-AXS). Frame integration and unit-cell refinement software was carried out with "SAINT+" (v6.22, Bruker AXS). Absorption corrections were applied by SADABS (v2.03, Sheldrick). Structures were solved by direct methods using SHELXS-97 (Sheldrick, 1997) and refined by full-matrix least squares using SHELXL-97 (Sheldrick, 1997). All non-hydrogen atoms were refined anisotropically. Hydrogen atoms were placed using a "riding model" and included in the refinement at calculated positions. In the case of the crystals of **6c**[OTf]·0.56CH_2Cl_2 diffraction was only observed upto an angle of 22.61° using Mo-Kα radiation which may be due to the disorder observed in the structural solution.

Acknowledgements

With thank the EPSRC and University of York for funding (DTA award to MJC).

Notes and references

1 (*a*) M. I. Bruce, *Chem. Rev.*, 1991, **91**, 197; (*b*) H. Werner, *J. Organomet. Chem.*, 1994, **475**, 45; (*c*) M. C. Puerta and P. Valerga, *Coord. Chem. Rev.*, 1999, **193–195**, 977; (*d*) Y. Wakatsuki, *J. Organomet. Chem.*, 2004, **689**, 4092; (*e*) V. Cadierno, M. P. Gamasa and J. Gimeno, *Coord. Chem. Rev.*, 2004, **248**, 1627; (*f*) A. B. Antonova, *Coord. Chem. Rev.*, 2007, **251**, 1521.

2 For recent references see: (*a*) D. B. Grotjahn, X. Zeng and A. L. Coosky, *J. Am. Chem. Soc.*, 2006, **128**, 2798; (*b*) D. B. Grotjahn, X. Zeng, A. L. Cooksy, W. S. Kassel, A. G. DiPasquale, L. N. Zakharov and A. L. Rheingold, *Organometallics*, 2007, **26**, 3385; (*c*) M. J. Cowley, J. M. Lynam and J. M. Slattery, *Dalton Trans.*, 2008, 4552; (*d*) J. M. Lynam, C. E. Welby and A. C. Whitwood, *Organometallics*, 2009, **28**, 1320; (*e*) D. B. Grotjahn, V. Miranda-Soto, E. J. Kragulj, D. A. Lev, G. Erdogan, X. Zeng and A. L. Cooksy, *J. Am. Chem. Soc.*, 2008, **130**, 20; (*f*) M. Bassetti, V. Cadierno, J. Gimeno and C. Pasquini, *Organometallics*, 2008, **27**, 5009.

3 (*a*) C. Bruneau and P. H. Dixneuf, *Acc. Chem. Res.*, 1999, **32**, 311; (*b*) B. M. Trost, M U. Frediksen and M. T. Rudd, *Angew. Chem., Int. Ed.*, 2005, **44**, 6630; (*c*) C. Bruneau and P. H. Dixneuf, *Angew. Chem., Int. Ed.*, 2006, **45**, 2176; (*d*) B. M. Trost and A McClory, *Chem.–Asian J.*, 2008, **3**, 164.

4 For reviews of this area see: (*a*) M. K. Whittlesey, in *Comprehensive Organometallic Chemistry III*, ed. R. H. Crabtree, D. M P. Mingos and M. I. Bruce, Elsevier, Oxford, U.K., 2006, vol. 6, chapter 6.12; (*b*) J. Gimeno and V. Cadierno in *Comprehensive Organometallic Chemistry III*, ed. R. H. Crabtree, D. M P. Mingos and M. I. Bruce, Elsevier, Oxford, U.K., 2006, vol. 6, chapter 6.15.

5 (*a*) F. Paul, B. G. Ellis, M. I. Bruce, L. Toupet, T. Roisnel, K. Costuas, J.-F. Halet and C. Lapinte, *Organometallics*, 2006, **25**, 649; (*b*) C. Bitcon and M. W. Whiteley, *J. Organomet. Chem.*, 1987, **336**, 385; (*c*) N. J. Long and C. K. Williams, *Angew. Chem., Int. Ed.*, 2003, **42**, 2586; (*d*) W. M. Khairul, M. A. Fox, N. N. Zaitseva, M. Gaudio, D. S. Yufit, B. W. Skelton, A. H. White, J. A. K. Howard, M. I. Bruce and P. J. Low, *Dalton Trans.*, 2009, 610.

6 (*a*) C. E. Powell and M. G. Humphrey, *Coord. Chem. Rev.*, 2004, **248**, 725; (*b*) M. A. Fox, R. L. Roberts, T. E. Baines, B. Le Guennic, J.-F. Halet, F. Hartl, D. S. Yufit, D. Albesa-Jov, J. A. K. Howard and P. J. Low, *J. Am. Chem. Soc.*, 2008, **130**, 3566; (*c*) M. A. Fox, R. L. Roberts, W. M. Khairul, F. Hartl and P. J. Low, *J. Organomet. Chem.*, 2007, **692**, 3277; (*d*) C.-Y. Wong, C.-M. Che, M. C. W. Chan, J. Han, K.-H. Leung, D. L. Phillips, K.-Y. Wong and N. Zhu, *J. Am. Chem. Soc.*, 2005, **127**, 13997; (*e*) N. Gauthier, N. Tchouar, F. Justaud, G. Argouarch, M. P. Cifuentes, L. Toupet, D. Touchard, J.-F. Halet, S. Rigaut, M. G. Humphrey, K. Costuas and F. Paul, *Organometallics*, 2009, **28**, 2253; (*f*) C. E. Powell, M. P. Cifuentes, J. P. Morrall, R. Stranger, M. G. Humphrey, M. Samoc, B. Luther-Davies and G. A. Heath, *J. Am. Chem. Soc.*, 2003, **125**, 602.

7 J. M. Lynam, *Dalton Trans.*, 2008, 4067.

8 M. J. Cowley, J. M. Lynam and A. C. Whitwood, *Dalton Trans.*, 2007, 4427.

9 M. I. Bruce and R. C. Wallis, *Aust. J. Chem.*, 1979, **32**, 1471.

10 M. I. Bruce and A. G. Swincer, *Aust. J. Chem.*, 1980, **33**, 1471.

11 H. Hamidov, J. C. Jeffery and J. M. Lynam, *Chem. Commun.*, 2004, 1364.

12 J. M. Lynam, T. D. Nixon and A. C. Whitwood, *J. Organomet. Chem.*, 2008, **693**, 3103.

13 (*a*) R. E. Hurd and B. R. Reid, *Nucleic Acids Res.*, 1977, **4**, 2747; (*b*) J. Pranata, S. G. Wierschke and W. L. Jorgensen, *J. Am. Chem. Soc.*, 1991, **113**, 2810.

14 V. Cadierno, M. P. Gamasa, J. Gimeno, J. Borge and S. García-Granda, *Organometallics*, 1997, **16**, 3178.
15 V. Cadierno, M. P. Gamasa, J. Gimeno, C. González-Bernardo, E. Pérez-Carreño and S. García-Granda, *Organometallics*, 2001, **20**, 5177.
16 K. Ogata, J. Seta, Y. Yamamoto, K. Kuge and K. Tatsumi, *Inorg. Chim. Acta*, 2007, **360**, 3296.
17 N. M. Kostic and R. F. Fenske, *Organometallics*, 1982, **1**, 974.
18 S.-H. Choi, I. Bytheway, Z. Lin and G. Jia, *Organometallics*, 1998, **17**, 3974.
19 W. Han Lam and Z. Lin, *J. Organomet. Chem.*, 2001, **635**, 84.
20 B. E. Boland-Lussier, M. R. Churchill, R. P. Hughes and A. L. Rheingold, *Organometallics*, 1982, **1**, 628.
21 K. Onitsuka, M. Nishii, Y. Matsushima and S. Takahashi, *Organometallics*, 2004, **23**, 5630.
22 (*a*) M. I. Bruce, Richard C. F. Gardner, F. Gordon and A. Stone, *J. Chem. Soc., Dalton Trans.*, 1976, 81; (*b*) M. I. Bruce, M. P. Cifuentes, M. G. Humphrey, E. Poczman, M. R. Snow and E. R. T. Tiekink, *J. Organomet. Chem.*, 1988, **338**, 237.
23 M. I. Bruce, C. Hameister, A. G. Swincer and R. C. Wallis, *Inorg. Synth.*, 1982, **21**, 78.
24 J. W. B. Cooke, R. Bright, M. J. Coleman and K. P. Jenkins, *Org. Process Res. Dev.*, 2001, **5**, 383.
25 *gNMR, version 5.0.5.0*, Ivory Software, 2005.

